



EARTHQUAKE SITE CLASS CHARACTERIZATION OF SEISMOGRAPH AND STRONG-MOTION STATIONS IN CANADA AND CHILE

S. Molnar⁽¹⁾, S. Braganza⁽²⁾, J. Farrugia⁽³⁾, G. Atkinson⁽⁴⁾, R. Boroschek⁽⁵⁾, C. Ventura⁽⁶⁾

⁽¹⁾ Assistant Professor, University of Western Ontario, Dept. Earth Sciences, London, ON, Canada, smolnar8@uwo.ca

⁽²⁾ M.Sc. Student, University of Western Ontario, Dept. Earth Sciences, London, ON, Canada, sbragan@uwo.ca

⁽³⁾ M.Sc. Student, University of Western Ontario, Dept. Earth Sciences, London, ON, Canada, jfarrugi@uwo.ca

⁽⁴⁾ Professor, University of Western Ontario, Dept. Earth Sciences, London, ON, Canada, gatkins6@uwo.ca

⁽⁵⁾ Associate Professor, University of Chile, Dept. Civil Engineering, Santiago, Chile, rborosch@ing.uchile.cl

⁽⁶⁾ Professor, University of British Columbia, Dept. Civil Engineering, Vancouver, BC, Canada, ventura@civil.ubc.ca

Abstract

Earthquake recording stations, seismographs and/or strong-motion instruments, located on underlying soils are generally installed without comprehensive knowledge or testing of the underlying geologic material in Canada and Chile. To remedy this issue, various *in situ* geophysical methods are applied to evaluate the underlying ground conditions at earthquake recording stations in Canada and Chile with the overall aim to develop a standard, systematic, and inexpensive procedure for earthquake site classification. The underlying geology at Canadian and Chilean earthquake recording stations is immensely variable and therefore comprehensive to this study's application. At central and southern Chilean strong-motion stations that recorded the 2010 M_W 8.8 Maule earthquake, boreholes were drilled to 30-80 m depth and various invasive methods (downhole velocity, laboratory bender element, and standard penetration testing) were performed, as well as passive (ambient vibration) array testing at surface. At northern Chilean strong-motion stations that recorded the 2014 M_W 8.2 Iquique earthquake, a combination of active (hammer-impact) and passive surface wave array testing was performed. Combination surface wave array testing is also performed at Canadian seismograph stations in Alberta (western Canada) and Ontario (eastern Canada). For all stations, spectral ratio analysis of ambient vibration and available earthquake recordings is performed. A database of each station's earthquake site classification according to the respective National Building Code in Canada and Chile is generated – both countries have adopted the six NEHRP (Natural Earthquake Hazard Reduction Program) site classification groupings (A-F) based primarily on the harmonic average shear-wave velocity over the upper 30 meters (i.e., V_{S30}) with slightly different bounds in v_{S30} per site class. Expansion or evolution of v_{S30} -based site classification to include spectral content (i.e., site period or peak frequency classifications) is included in this study.

Keywords: earthquake site classification, amplification, v_{S30} , seismic networks.



1. Introduction

In Canada and Chile, earthquake recording stations are typically installed without proper site characterization, i.e., *in situ* measurement of underlying ground conditions such as velocity depth profiling. Weak-motion seismograph stations, as part of a national seismic network, are preferentially installed on firm to hard bedrock ground conditions in an effort to minimize variable site conditions amongst stations; the same regional velocity model is used to locate earthquakes. In contrast, strong-motion accelerographs are typically installed on a variety of ground conditions to capture anticipated high(er) earthquake ground shaking on softer soils or at near-source distances.

Recorded earthquake ground shaking is used to develop ground-motion prediction equations (GMPE) and resulting variability due to different site conditions amongst stations must be reduced. This is typically accomplished by grouping or binning stations into six categories of earthquake site classification; Natural Earthquake Hazard Reduction Program (NEHRP) site classification designations based on the time-averaged shear-wave velocity (V_S) over the upper 30-meters (V_{S30}) at a site has been adopted by Canadian building codes in 2005 and Chilean building codes following the 2010 M8.8 Maule, Chile, earthquake. Hence, determination of V_S depth profiles and V_{S30} at earthquake recording stations in Canada and Chile are necessary for inclusion of these station's records in GMPE databases.

Empirical earthquake recordings enable characterization of a site's earthquake response behavior; an average amplification spectrum (transfer function) is determined via soil-to-bedrock or horizontal-to-vertical spectral ratio (HVSR) analysis of the earthquake recordings. However, problems arise when empirical earthquake recordings are lacking due to low seismicity rates, triggering of strong-motion instruments from large earthquakes is rare, or only recordings at soil sites are obtained. Microtremor (ambient vibration) recordings may provide earthquake site characterization in lieu of earthquake recordings via two main methods: microtremor HVSR analysis to obtain the site's average amplification spectrum, and microtremor array measurements to obtain surface wave dispersion data to invert for the site's V_S profile(s) and/or V_{S30} site classification.

This paper documents recent earthquake site characterization studies conducted at seismograph and strong-motion stations in Canada and Chile. Each country spans ~6,000 km and therefore significant geologic variability is sampled herein.

2. Alberta, Canada

Significant growth in seismic monitoring has occurred in Alberta over the past few decades with recognition of increased seismic activity [1] related to induced seismicity from hydraulic fracking processes [2]. Station installation is to provide adequate coverage for natural and induced earthquake location purposes; hence, stations in Alberta are installed on a variety of ground conditions without proper geotechnical characterization. Overburden thickness in central Alberta is in excess of 100 m, consisting of layered Quaternary fluvial deposits and glaciogenic materials, as well as post-glacial sediments [3, 4, 5], demonstrating the potential for occurrence of broad-band and resonance amplification; thin soil or bedrock stations generally occur in the Rocky Mountain foothills in southwest Alberta. Figure 1a presents seismograph station locations used currently in the Alberta site characterization study in conjunction with hypocentral locations of earthquakes (Sept. 2013 - Feb. 2016). The work currently being done to characterize site amplification at seismograph stations in Alberta thus has profound relevance to current inquiries and research interests of industry and academia and implications for seismic hazard analyses.

To date, efforts to understand the role geology, overburden thickness (depth to bedrock) and soil stiffness have on the observed ground motions from seismograph stations have consisted of analyses on earthquake data derived horizontal-to-vertical spectral ratios (HVSR) from acceleration response spectra. A sample subset of HVSRs from Alberta seismograph stations are presented in Figure 1. Farrugia and Atkinson [6] determine an average amplification factor on the order of ~0.3 log base 10 units at TransAlta seismograph stations (Figure 1). Recently, seismograph stations from the Canadian National Seismic Network (CNSN) and the Regional Alberta Observatory for Earthquake Studies Network (RAVEN) have been included in the study, such as WALA in



Figure 1b, which shows little to no amplification. In the future, earthquake records from the Canadian Rockies and Alberta Network (CRANE) will be included bringing the total number of seismograph stations included in the study to 66. Table 1 lists select seismograph stations currently in the site characterization study along with quantities for pertinent site variables and site classes assigned using site period [7], quarter-wavelength [8], and topographic proxy [9] methods.

Table 1 demonstrates the variability in earthquake site classification via different methods for the select Alberta seismograph stations. Hence, an *in situ* field campaign will occur in July 2016 to supply necessary V_S depth profiles for seismograph stations through the inversion of dispersion curves obtained through surface-wave testing and ambient noise array methods. These measurements will allow for a site-specific estimation of V_{S30} , and subsequently site class according to the provisions set by NEHRP and adopted by Canadian building code standards. Combining this with publicly available datasets, such as bedrock depth shown in Figure 1a, the goal is to generate parameterized site amplification functions through the correlation of site descriptor variables such as surficial geology, depth to bedrock, V_{S30} , and site period with observed ground motions.

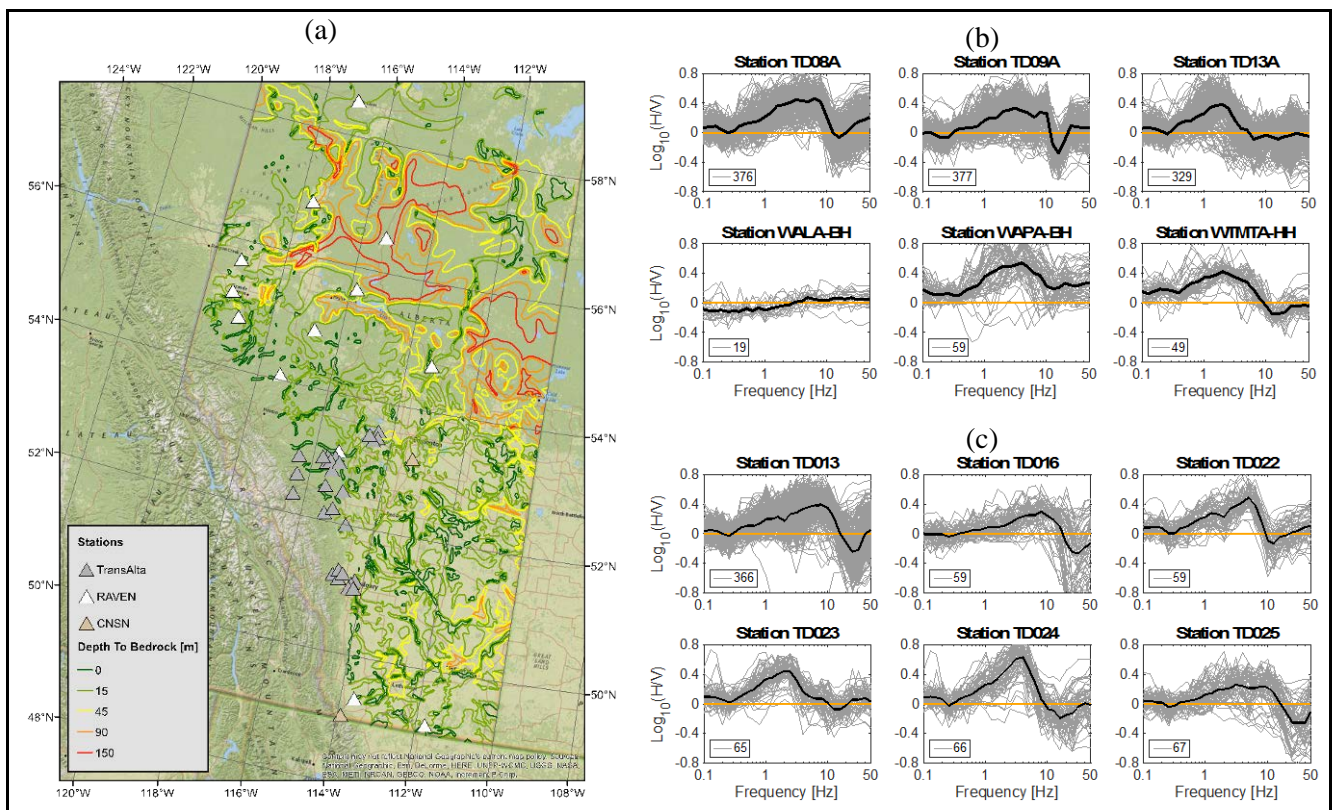


Figure 1. (a) Seismograph station locations shown in comparison to bedrock depth contours (Alberta Geological Survey, Map 227 [10]). (b) Select Alberta station average HVSR. The gold line represents unity; thin grey lines are individual HVSR and illustrate the variability in earthquake site response for that station; number of individual HVSRs is given in legend; the thick black line is the station average HVSR.



Table 1. Select Alberta seismograph stations and corresponding earthquake site classification designations.

| Station Name | Lat. [°N] | Long. [°E] | Depth to Bedrock (H) [m] | H/V Peak Freq. (f_{peak}) [Hz] | f_{peak} Site Class* | Topographic Proxy ⁺ | | Earthquake H/V | |
|--------------|-----------|------------|--------------------------|------------------------------------|------------------------|--------------------------------|--------------------|-----------------------------|--------------------|
| | | | | | | V_{S30} [m/s] | Site Class (NEHRP) | $V_z = 4 * H * f_{peak} \%$ | Site Class (NEHRP) |
| TD013 | 52.518 | -115.024 | 5.3 | 3 | SC II | 760 | C | 63.2 | E |
| TD016 | 51.210 | -114.836 | 5.0 | 5 | SC II | 292 | D | 100.0 | E |
| TD022 | 51.177 | -114.229 | 13.5 | 5 | SC II | 357 | D | 270.4 | D |
| TD023 | 51.111 | -114.305 | 14.1 | 2 | SC III | 760 | C | 113.0 | E |
| TD024 | 51.048 | -114.362 | 13.6 | 4 | SC II | 358 | D | 218.0 | D |
| TD025 | 51.161 | -114.676 | 5.0 | 2.5 | SC III | 657 | C | 50.0 | E |
| TD08A | 52.948 | -115.278 | 2.1 | 3 | SC II | 760 | C | 24.7 | E |
| TD09A | 52.925 | -116.390 | 1.6 | 2.5 | SC III | 760 | C | 15.9 | E |
| TD13A | 52.008 | -114.768 | 12.5 | 1.8 | SC III | 394 | C | 90.0 | E |
| WALA | 49.059 | -113.912 | 0.0 | | | 760 | C | | |
| WAPA | 55.183 | -119.254 | 14.6 | 3 | SC II | 655 | C | 175.3 | E |
| WTMTA | 55.694 | -119.240 | 3.8 | 2 | SC III | 760 | C | 30.6 | E |

f_{peak} denotes peak frequency; *[7]; ⁺Stable Craton [9]; % [8].

3. British Columbia, Canada

Site response at ~106 strong-motion stations in British Columbia was determined using HVSR analysis from earthquake and/or microtremor recordings [11, 12, 13, 14]. Demonstration in the utility of single-sensor microtremor HVSR analysis as a proxy for earthquake site response in Canada was first conducted at strong-motion stations in Victoria (Figure 2a) [13]. Validation in microtremor HVSR peak frequency and amplitude in comparison to earthquake spectral ratios provided significant opportunity to use microtremor techniques as an earthquake site amplification reconnaissance tool in British Columbia, e.g., [14, 15]. *In situ* geophysical site characterization resulting in estimated shear-wave velocity profiles has been performed at a handful of these British Columbia strong-motion stations.

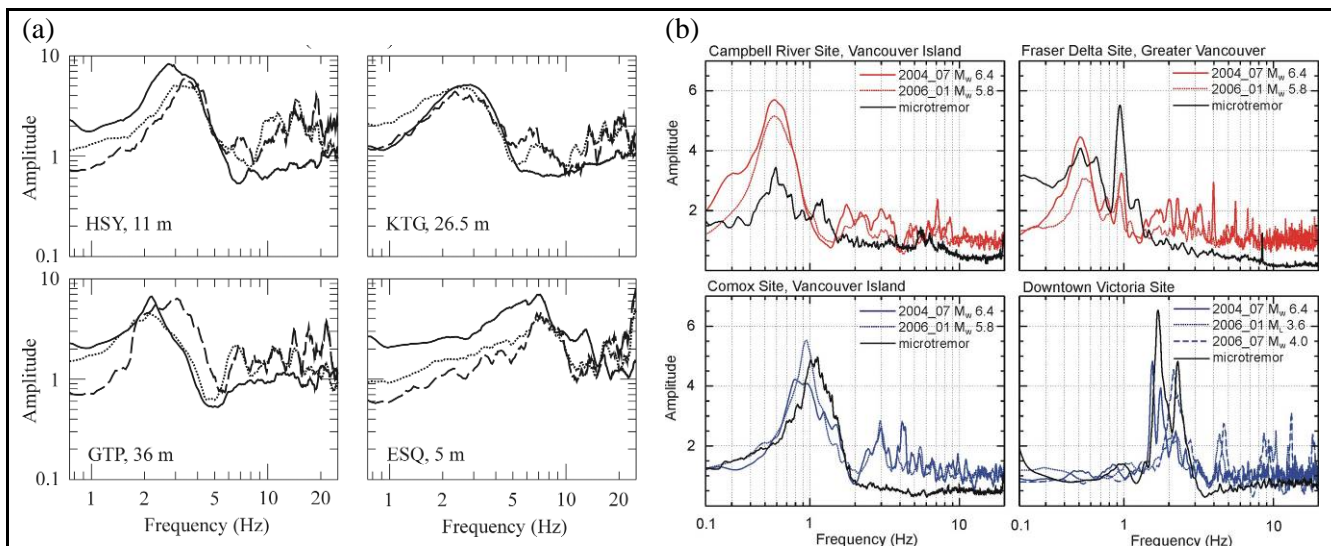


Figure 2. (a) Comparison of earthquake soil-to-bedrock (dashed line) and H/V (dotted line) spectral ratios with average microtremor HVSR (solid line) at four strong-motion stations in Greater Victoria; modified from [13]. Station code and soil thickness reported in bottom left. (b) Comparison of earthquake and microtremor HVSRs at four strong-motion stations throughout British Columbia; modified from [14].



4. Ontario, Canada

In southern Ontario, the sediment layers which overlie glaciated bedrock produce strong and highly variable site response. For this region, HVSRs from acceleration response spectra are used as the indicator variable by which to characterize the salient characteristics of site response. This is modeled using two key descriptive variables that are readily obtainable: (i) peak resonant frequency (f_{peak}), as determined from the peak in the earthquake HVSR or estimated from sediment depth; and (ii) overall sediment age and material composition (proxy for stiffness). These variables are used to create a preliminary model of site amplification that can be used in the development of ground-motion prediction equations (GMPEs) and in regional-scale ShakeMap-type applications [16].

The key to the site characterization is the relationship between f_{peak} and sediment thickness (depth-to-bedrock), which is derived using HVSR data from earthquakes in the region and geological information available online. Furthermore, a correlation is made between surficial sediment type and peak amplitudes (A_{peak}) of response. HVSR spectral shapes are found to be associated with four main site categories, which in decreasing order of stiffness are: bedrock, glaciated till, sand/clay, and organic sediment or fill. The peak amplitudes of response are generally shown to increase as stiffness decreases, ranging from a factor of about 1 for seismograph stations on bedrock, to just under 10 on organic sediment. Figure 3a shows the earthquake HVSRs for seven sand/clay seismograph sites, which is then averaged and normalized to derive a modelled site amplification function representative of sand/clay sites in Ontario. This is accomplished for each of the four site categories and provides a set of generic site amplification curves for Ontario seismograph stations (Figure 3b). Overall, average amplification functions on sediments in eastern Canada are much sharper and more pronounced than would be suggested by typical amplification functions that are applied in western North America [16].

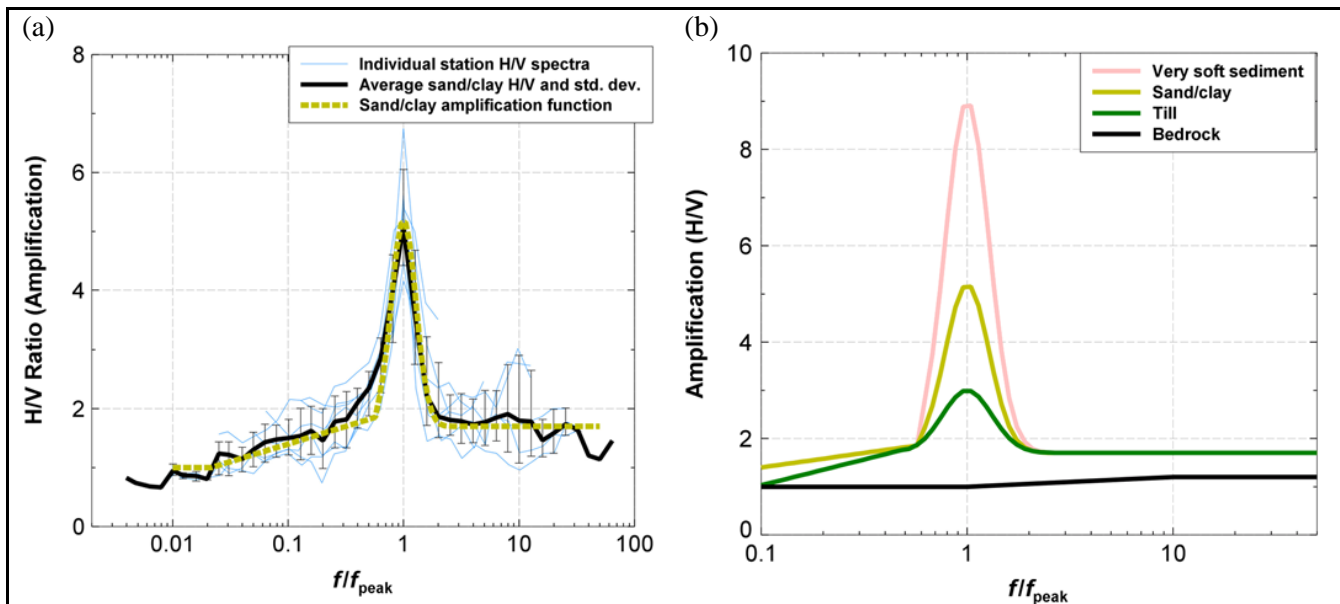


Figure 3. (a) Individual earthquake HVSRs at 7 seismograph stations on sand/clay (normalized to f_{peak}) with the weighted average H/VSR curve and derived amplification function. (b) Amplification functions of four different site categories for seismograph sites. Modified from [16].

An *in situ* microtremor field campaign at Ontario seismograph stations is underway to validate microtremor HVSR application in eastern Canada. Motazedian et al. [17] document a nonlinear relationship in f_{peak} between microtremor HVSRs and theoretical fundamental peak frequency based on known glaciomarine sediment thickness at borehole sites in the Ottawa valley, northeastern Ontario.

5. Central and Southern Chile

In Chile, microtremor measurements have been performed primarily at strong-motion stations in the Santiago metropolitan area for validation with earthquake recordings [18, 19, 20, 21], but also for earthquake site effect assessment in Santiago [22, 23, 24], Concepcion [25], and Lloleco [26]. Prior to the 2010 M_w 8.8 Maule earthquake, no site-specific subsurface information was available for Chilean strong-motion stations outside of Santiago. As such, the University of Chile (UCH) Research and Material Testing Institute (Instituto de Investigación y Ensayo de Materiales, IDIEM) Civil Engineering Department (Departamento de Ingeniería Civil, DIC) conducted a post-earthquake invasive borehole testing campaign at 11 strong-motion stations in central and southern Chile (Figure 4) [27]. The UCH-IDIEM-DIC invasive testing campaign provides a detailed comprehensive assessment of the subsurface column of drilled material at each strong-motion station. Conversely, a rather crude non-invasive field testing campaign was performed at these same 11 Chilean strong-motion stations by the first author during a postdoctoral fellowship at the University of British Columbia (UBC) Earthquake Engineering Research Facility (EERF), Vancouver, British Columbia, Canada. The UBC-EERF campaign was optimized for efficiency and budget by minimization of equipment, personnel, and time. The invasive testing results were not made available to the first author until the microtremor data were processed and inverted for V_S structure, i.e. a blind test. The comparison of invasive and non-invasive V_S -profiling methods is performed in terms of the average relative difference in V_S for particular depth ranges and the resulting site classification based on V_{S30} . The non-invasive microtremor recordings, in combination with available earthquake recordings at the 11 Chilean strong-motion stations, allows for a second and independent evaluation of site classification based on predominant site period.

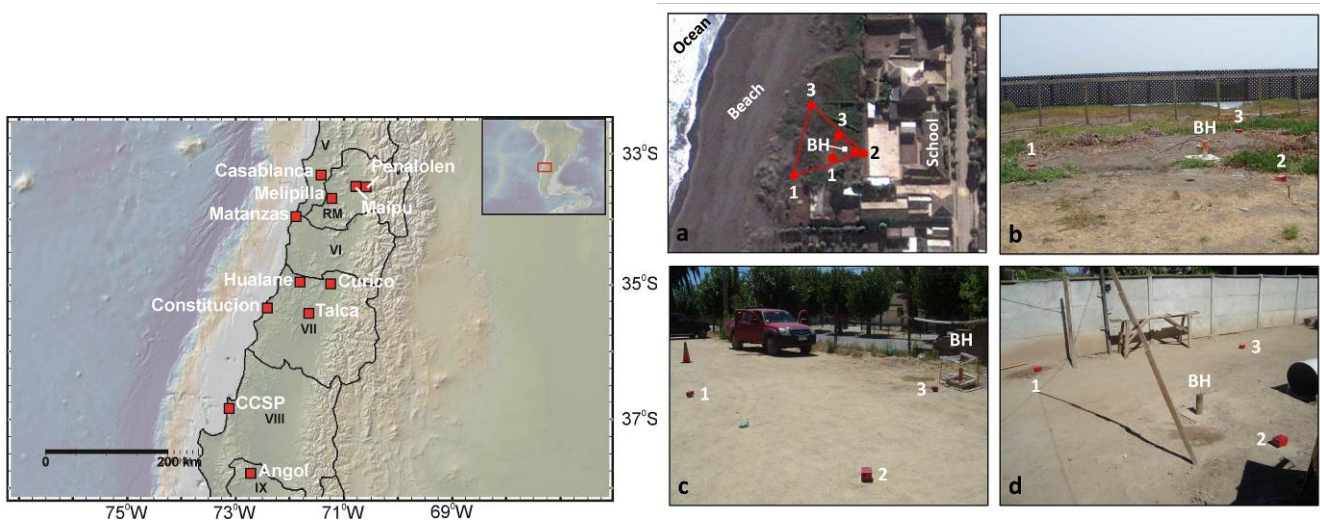


Figure 4. (Left) Locations of 11 investigated Chilean strong-motion stations (squares) with regional districts (V-IX) marked by solid lines. (Right) Overview map of 5-m and 15-m equilateral triangular arrays at Matanzas. Each sensor is numbered and marked by a circle and the borehole (BH) location is marked by a square. (b) Photo of 5-m array at three different station sites. Modified from [27].

Two types of V_S profiling are accomplished. First, a suite of invasive methods were performed by UCH-IDIEM-DIC, including downhole compression- and shear-wave velocity, standard penetration testing (SPT) N_{60} blowcounts, and laboratory bender element (BE) V_S measurements. Second, non-invasive passive-source microtremor array testing was performed by UBC-EERF at each drilled borehole location to obtain dispersion data for probabilistic inversion of V_S profiles. Figure 5 presents the mean V_S profile and 95% highest probability density (HPD) V_S profile credibility interval determined from probabilistic inversion for each station. For all stations, V_S is generally well resolved in the upper 30-m, which is the target depth of the field procedure and building code site classification. The mean and one standard deviation of the invasive V_S datasets is calculated for comparison with the non-invasive probabilistic inversion results shown in Figure 5. For a variety of geological conditions, excellent to good agreement is obtained between invasive and non-invasive V_S structure

at five stations over the entire borehole length and in the uppermost layer at three stations. The average relative difference in V_s between methodologies is 10% for soil layers and 30% for base rock.

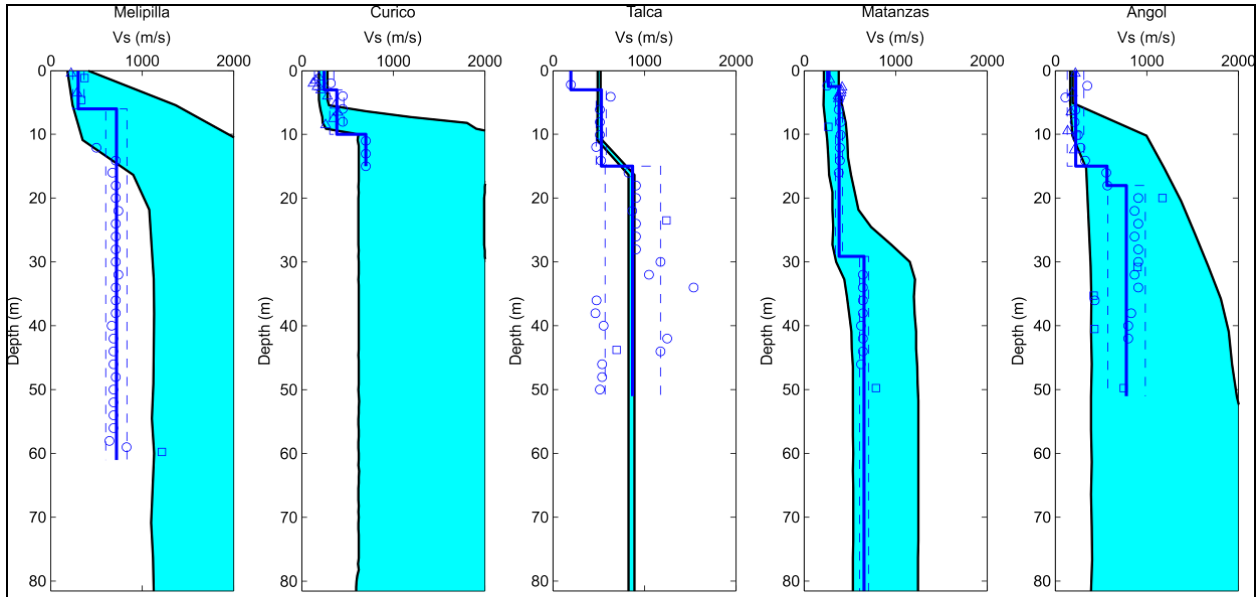


Figure 5. For 5 select sites, probabilistic inversion results shown by shaded area are compared with the mean invasive-methods V_s profile and one standard deviation estimates shown by solid and dashed lines, respectively. Modified from [27].

Figure 6 shows each earthquake and average microtremor Fourier H/V velocity spectral ratios for 6 select strong-motion stations. For stations with multiple earthquake recordings, earthquake ratios are relatively consistent between events. The average microtremor H/V ratio for the 11 stations displays either a clear site period or is rather flat, indicative of stations dominated by soft/fine-grained and stiff/coarse-grained sediments, respectively, as observed at other sites in Chile [22, 28, 29, 30].

Stations with high V_{s30} values generally exhibit a short predominant period (< 0.4 sec) whereas stations with low V_{s30} values exhibit a longer predominant period (≥ 0.4 sec), as expected. The stiffest coarse-grained V_{s30} -based site class B stations (Melipilla, Talca, Curico) are readily distinguished by earthquake and microtremor H/V ratios; short site periods and/or flat microtremor ratios. For all other softer site class C and D stations, observed site period is more variable.

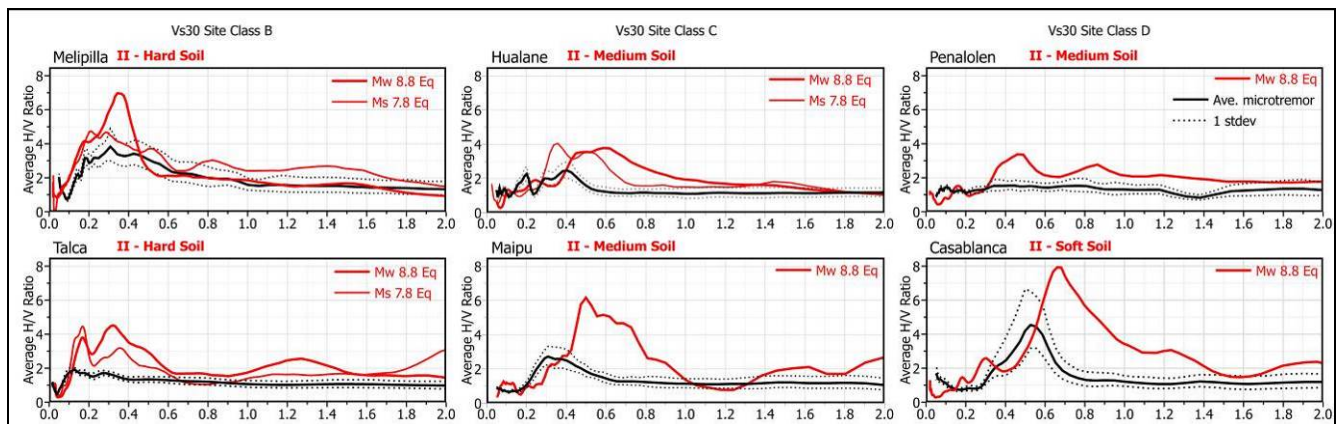


Figure 6. Average Fourier velocity H/V spectral ratios calculated from earthquake (coloured lines) and microtremor (black line with one standard deviation denoted by dashed lines) recordings for 6 select stations. Stations organized by V_{s30} site classification. Modified from Molnar et al. 2015 [27].



6. Northern Chile

On April 1, 2014, a M_w 8.2 earthquake struck off the coast of northern Chile, northwest of Iquique. A joint UCH-DIC and UBC-EERF (see southern Chile case study above) noninvasive field campaign for seismic site characterization was performed at 17 strong-motion stations in northern Chile (Figure 7). Surface seismic testing was performed by two students (one each from UCH-DIC and UBC-EERF) over ten days from June 23 to July 2, 2014. A total of six Tromino sensors were used; four from UBC-EERF and two from UCH-DIC. Three different types of tests were performed at each site: single-sensor MHVSR measurements, circular microtremor (passive-source) arrays, and linear hammer-impact (active-source) arrays (i.e., Multi-channel Analysis of Surface (Rayleigh) Waves, MAS_RW). Active-source surface wave testing was added to this northern Chile campaign in comparison to the earlier southern Chile campaign described above, as sediments are generally shallower and/or stiffer in northern Chile. The single MHVSR measurements were of 15-minute duration and performed at various locations around the strong-motion station site to confirm consistency in peak frequency. Microtremor arrays consisted of five sensors symmetrically surrounding a sixth central sensor with three different radius setups (typically 5, 10, and 15 m) to resolve lower frequency surface wave dispersion. One or more linear MAS_RW arrays (between 2 to 7 m sensor spacing) are accomplished at each site to resolve higher frequency dispersion data; active-source hammer impact occurred at each end of the line at three different offset distances. A similar noninvasive microtremor and surface wave testing campaign was performed by Becerra et al. [31] at 148 sites around Arica and Iquique to establish urban seismic microzonation mapping of the two cities based on V_{S30} and f_{peak} as well as in comparison to observed damage at four locations in Iquique and Alto Hospicio [32].



Figure 7. Locations of 17 investigated strong-motion stations in northern Chile.

All field measurements accomplished with the three-component Tromino sensors were loaded into a Geopsy database for dispersion and MHVSR analysis. For the 17 strong-motion stations, approximately half the stations exhibit flat (8 stations) or peaked (9 stations) MHVSR response. At 9 stations, dispersion data is extracted from the active- and passive-source surface wave field data for inversion. Hence, the same general field procedure did not produce surface wave dispersion results viable for inversion at 8 stations; generally the same stations with flat MHVSR response indicative of stiff rock-like ground conditions. For brevity, preliminary inversion results for two end-member earthquake site characterization case studies are presented here.



A flat MHVSR response is observed (Fig. 8a) at the Iquique airport station, 40 km south of Iquique. Rayleigh phase velocities of 400-1000 m/s at 30-200 Hz are obtained (Fig. 8b). Bayesian inversion of the dispersion data (Molnar et al. 2010) determines relatively high V_S (Fig. 8b) and V_{S30} of 985 m/s (74 m/s standard deviation) corresponding to Chilean site class A, rocks or cemented soil.

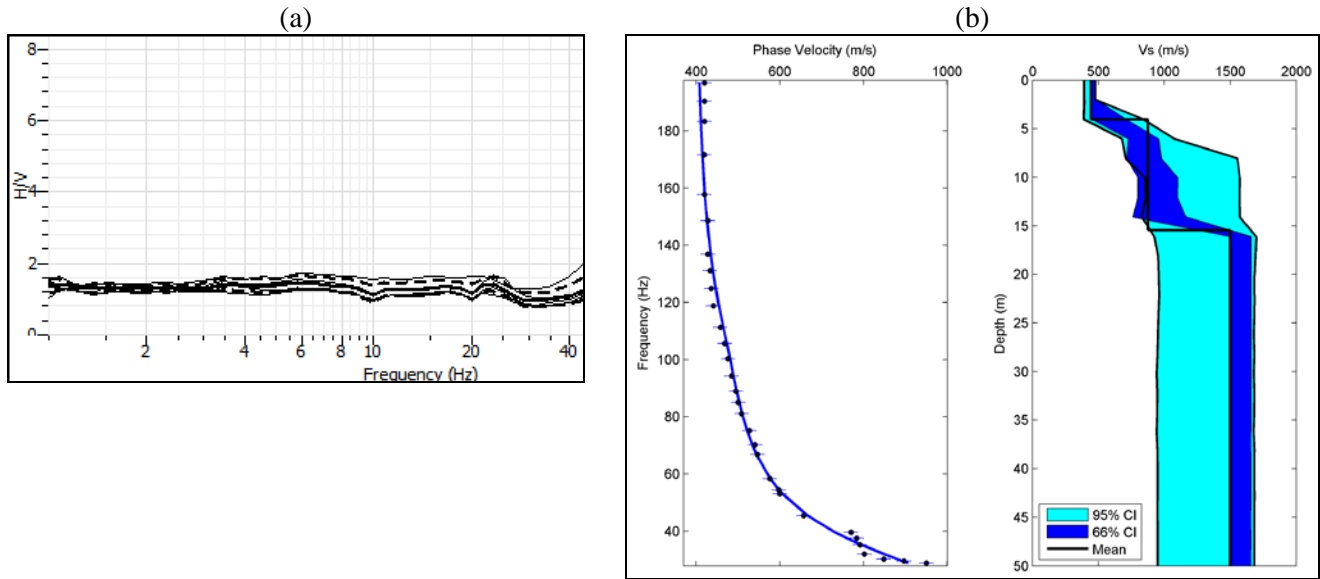


Figure 8. Iquique airport station. (a) Average MHVSR for each array sensor and site average MHVSR (thick solid line) with one standard deviation (dashed lines). (b) (Left) Dispersion data (filled circles) shown with dispersion solution (solid line) from maximum *a posteriori* model. (Right) Inverted V_S probability distribution (shaded area; CI in legend refers to highest-probability density credibility interval) with mean V_S profile (solid line).

In contrast, a single peaked MHVSR response at ~ 2.2 Hz (Fig. 9a) is observed at the Pozo Almonte strong-motion site, 50 km east of Iquique. Lower Rayleigh phase velocities of 200-600 m/s are determined at 1-90 Hz (Fig. 9b). Bayesian inversion of the dispersion curve determines relatively moderate V_S (Fig. 9b) and V_{S30} of 378 m/s (16 m/s standard deviation), corresponding to Chilean site class C, dense or firm soils.

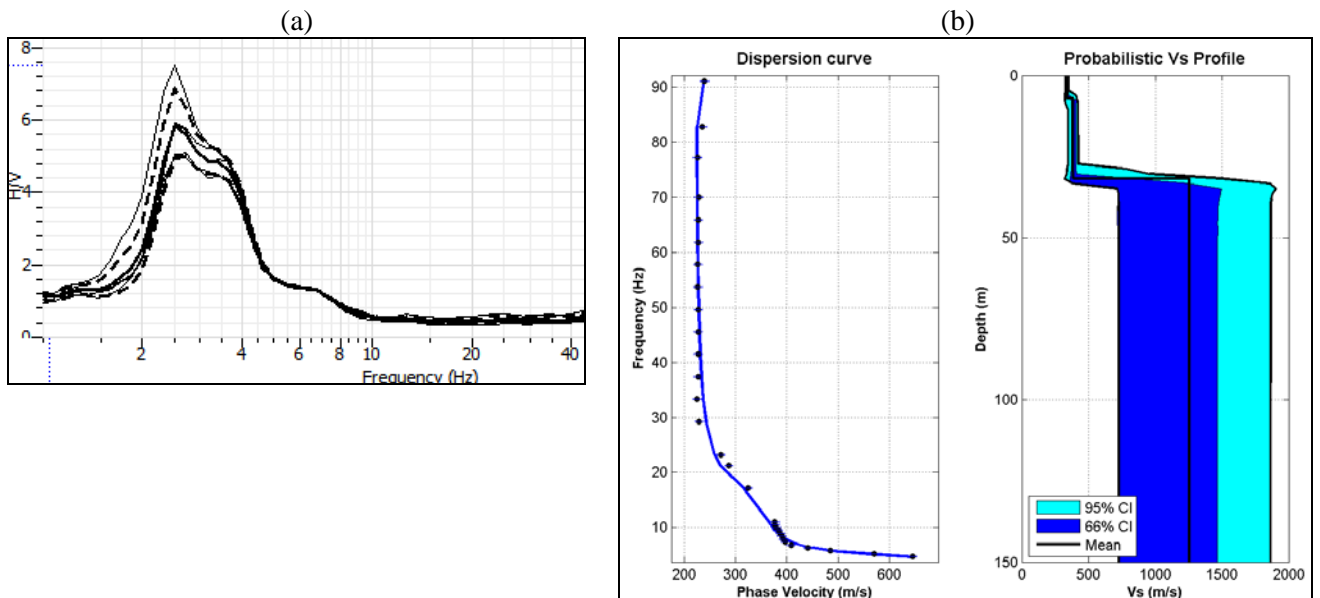


Figure 9. As above for Pozo Almonte station.



7. Summary

This paper summarizes ongoing efforts to determine and characterize earthquake site response at seismograph and strong-motion stations across Canada and Chile. Microtremor and earthquake HVSR analysis is used to determine site classification via peak resonant frequency or site period (e.g., Alberta and southern Chile case studies) as well as the full amplification spectrum (e.g., Ontario case study). Surface wave array testing, including passive microtremor and/or active hammer-impact seismic sources, provide dispersion data to invert for V_S profiles and V_{S30} -based site classification (e.g., southern and northern Chile case studies). Canadian and Chilean building codes adopted V_{S30} -based earthquake site classification in 2005 and 2010, respectively.

7. Acknowledgements

We acknowledge the data compilation and processing work of Karen Assatourians (Western University) that enables the presented Alberta and Ontario research. Thanks to Manuel Archila (formerly UBC-EERF), Victor Contreras-Luarte (UCH), and Oscar Jimenez (IDIEM) for help with southern Chile field collection. For northern Chile, thanks to Steve McDonald and Joaquin Bilbao (UCH-DIC) for field data collection and Amaia Martinez Martinez (UBC-EERF) for data processing. Funding provided by Natural Sciences and Engineering Research Council (NSERC), and Universidad de Chile.

8. References

- [1] Eaton, D., 2014. Alberta Telemetered Seismograph Network (ATSN): Real-time Monitoring of Seismicity in Northern Alberta. CSEG Recorder, p. 30-33.
- [2] Atkinson, GM, DW Eaton, H Ghofrani, D Walker, B Cheadle, R Schultz, R Shcherbakov, K Tiampo, J Gu, Y Liu, M van der Baan, H Kao (2016). Hydraulic fracturing and seismicity in the Western Canada Sedimentary Basin, *Seis. Res. Lett.*, 87, 631-647.
- [3] Fenton, M.M., Waters, E.J., Pawley, S.M., Atkinson, N., Utting, D.J. and Mckay, K., 2013. Surficial geology of Alberta; Alberta Energy Regulator, AER/AGS Map 601, scale 1:1 000 000.
- [4] Price, R.A., 2013. Chapter 2: Cordilleran Tectonics and the Evolution of the Western Canada Sedimentary Basin; in *Geological Atlas of the Western Canada Sedimentary Basin*, G.D. Mossop and I. Shetsen (comp.), Canadian Society of Petroleum Geologists and Alberta Research Council, URL <http://www.ags.gov.ab.ca/publications/wcsb_atlas/atlas.html>, [October 22, 2015].
- [5] MacCormack, K.E., Atkinson, N. and Lyster, S., 2015. Sediment thickness of Alberta, Canada; Alberta Energy Regulator, AER/AGS Map 603, scale 1:1 000 000.
- [6] Farrugia, J., and Atkinson, G., 2015. A preliminary evaluation of site amplification in Alberta, Undergraduate Geophysics Thesis, Western University, London, Ontario, Canada, 66 p.
- [7] Zhao, J.X., Irikura, K., Zhang, J., Fukushima, Y., Somerville, P.G., Sanao, A., Ohno, Y., Oouchi, T., Takahashi, T., and Ogawa, H. 2006. An empirical site-classification method for strong-motion stations in Japan using H/V response spectral ratio; *Bull., Seis. Soc. Am.*, Vol. 96, No. 3, 914-925.
- [8] Joyner WB, RE Warrick & TE Fumal, 1981. The effect of Quaternary alluvium on strong ground motion in the Coyote Lake, California, earthquake of 1979, *Bull. Seis. Soc. Am.*, 71, 1333-1349.
- [9] Wald, D. J., and T. I. Allen (2007). Topographic slope as a proxy for seismic site conditions and amplification, *Bull., Seism. Soc. Am.*, Vol. 97, No. 5, 1379-1395.
- [10] Pawlowicz, JG, and MM Fenton (1995). Drift thickness of Alberta, AGS Map 227. http://www.ags.aer.ca/document/MAP/MAP_227.pdf; last accessed May 30, 2016.
- [11] Cassidy, J. F., S. Molnar, G. C. Rogers, T. Mulder, and T. E. Little (2003). Canadian strong ground motion recordings of the 28 February, 2001 MW 6.8 Nisqually (Seattle-Olympia), Washington, earthquake, Geological Survey of Canada, Open File Report 1737, 91 pp.
- [12] Molnar, S., J. F. Cassidy, and S. E. Dosso. (2004). Site response in Victoria, BC from spectral ratios and 1D modeling, *Bull. Seism. Soc. Am.* 94, no. 3, 1109–1124.



- [13] Molnar, S., and Cassidy, J.F. (2006). A comparison of site response techniques using earthquakes and microtremors, *Earthquake Spectra*, 22, 169-188.
- [14] Molnar, S., JF Cassidy, PA Monahan, T Onur, C Ventura, and A Rosenberger, 2007. Earthquake site response studies using microtremor measurements in southwestern British Columbia, *Proceedings 9th Canadian Conference of Earthquake Engineering*, Ottawa, Ontario, Canada.
- [15] Molnar, S., C Ventura, WDL Finn, H Crow, T Stokes, P Lapcevic, and D Paradis, 2014. Regional seismic hazard assessment for small urban centres in western Canada, *Proceedings 10th National Conference in Earthquake Engineering*, Anchorage, Alaska.
- [16] Braganza, S, Atkinson, G, Ghofrani, H, Hassani, B, Chouinard, L, Rosset, P., Motazedian, D., and J. Hunter, (accepted). Modeling site amplification in eastern Canada on a regional scale, *Seismological Research Letters*.
- [17] Motazedian D, Khareshi Banab K, Hunter JA, Sivathayalan S, Crow H, and Brooks, G. 2011. Comparison of Site Periods Derived from Different Evaluation Methods; *Bulletin of the Seismological Society of America*, Vol. 101, No. 6, pp. 2942–2954, December 2011, doi: 10.1785/0120100344.
- [18] Toshihawa, T., M. Matsuoka, and Y. Yamazaki, 1996. Ground-motion characteristics in Santiago, Chile, obtained by microtremor observations, in *Proceedings, Eleventh World Conference on Earthquake Engineering*, Acapulco, Mexico, Paper 1764.
- [19] Cruz, E. F., R. Riddell, L. Fernandez, and D. Valdivia, 2000. A study of site amplification effects in Santiago based on earthquake records obtained from the SMASCH array, in *Proceedings, 12th World Conference on Earthquake Engineering*, Auckland, New Zealand.
- [20] Verdugo, R., and C. Pasten, 2007. Observation of seismic amplification on subductive environment, in *Proceedings, Fourth International Conference on Earthquake Geotechnical Engineering*, Thessaloniki, Greece, Paper 1462.
- [21] Leyton, F., and S. Ruiz, 2011. Comparison of the behaviour of site from strong motion data of 1985 Central Chile earthquake (MW 7.8) and microtremor measurements, in *Proceedings, Fifth International Conference on Earthquake Geotechnical Engineering*, Santiago, Chile, Paper CBSLR.
- [22] Bonnefoy-Claudet, S., S. Baize, L. F. Bonilla, C. Berge-Thierry, C. Pasten, J. Campos, P. Volant, and R. Verdugo, 2009. Site effect evaluation in the basin of Santiago de Chile using ambient noise measurements, *Geophysical Journal International* 176, 925-937.
- [23] Bonnefoy-Claudet, S., F. Leyton, S. Baize, C. Berge-Thierry, L. F. Bonilla, and J. Campos, 2008. Potentiality of microtremor to evaluate site effects at shallow depths in the deep basin of Santiago de Chile, in *Proceedings, Fourteenth World Conference on Earthquake Engineering*, Beijing, China.
- [24] Pilz, M., S. Parolai, F. Leyton, J. Campos, and J. Zschau, 2009. A comparison of site response techniques using earthquake data and ambient seismic noise analysis in the large urban areas of Santiago de Chile, *Geophysical Journal International* 178, 713-728.
- [25] Ramirez, P., and J. Vivallos, 2009. Microzonificación sísmica de la ciudad de Concepción-Chile, in *Proceedings, XII Congreso Geológico Chileno*, Santiago, Chile, S3_018.
- [26] Verdugo, R., 2009. Amplification phenomena observed in downhole array records generated on a subductive environment, *Physics of the Earth and Planetary Interiors* 175, 63-77.
- [27] Molnar, S., CE Ventura, R Boroschek, M Archila (2015). Site characterization at Chilean strong-motion stations: Comparison of downhole and microtremor shear-wave velocity methods, *Soil Dyn. Earth. Eng.*, 79, 22-35.
- [28] Leyton, F., S. Ruiz, S. A. Sepúlveda, J. P. Contreras, S. Rebolledo, and M. Astroza, 2013. Microtremors' HVSR and its correlation with surface geology and damage observed after the 2010 Maule earthquake (MW 8.8) at Talca and Curicó, Central Chile, *Engineering Geology* 161, 26-33.
- [29] Sekiguchi, T., N. Pulido, G. Shoji, J. Alba, and F. Lazares, 2011. Strong ground motions and site effects of the 2010 Chile earthquake, in *Proceedings, Eighth International Conference on Urban Earthquake Engineering*, Tokyo, Japan.
- [30] Leyton, F., G. Montalva, and P. Ramirez, 2011. Towards a seismic microzonation of Concepción urban area based on microtremors, surface geology, and damage observed after the Maule 2010 earthquake, *First Results*, in *Proceedings, Fourth IASPEI/IAEE International Symposium, Effects of surface geology on seismic motion*, University of California Santa Barbara.



- [31] Becerra, A., L. Podestá, R. Monetta, E. Sáez, F. Leyton, and G. Yañez (2015). Seismic microzoning of Arica and Iquique, Chile, *Natural Hazards*, 79, 567-586.
- [32] Becerra, A., E. Sáez, L. Podestá, and F. Leyton (2016). The 2014 earthquake in Iquique, Chile: Comparison between local soil conditions and observed damage in the cities of Iquique and Alto Hospicio, *Earthquake Spectra*, preprint.